

## Measurement of impedance of individual metallic carbon nanotubes

J. Obrzut<sup>1</sup>, K. Migler<sup>1</sup>, L. F. Dong<sup>2,3</sup> and J. Jiao<sup>2</sup>

<sup>1</sup>Polymers Division, National Institute of Standards and Technology, Gaithersburg, MD 20899.

<sup>2</sup>Physics Department Portland State University, Portland, Oregon 97207.

<sup>3</sup>Department of Physics, Astronomy and Materials Science, Missouri State University, Springfield, MO 65897.

E-mail: jano@nist.gov

**Abstract** – We describe impedance measurements of individual single wall carbon nanotubes (SWNTs) in the frequency range of 40 Hz to 100 MHz. The tubes were assembled on the active channel of field effect transistor (FET) structures from aqueous suspension using dielectrophoresis. The FET channels were made by using photo-lithography. We utilized a resistance-capacitance (RC) lumped element circuit model to describe the observed impedance of the tubes and the corresponding contact resistance. At the low frequency limit the impedance is frequency independent and equivalent to the real resistance. In the high frequency range we observe a sharp conductor-insulator transition at a crossover frequency, above which the circuit response becomes capacitive. The extracted SWNT capacitance,  $C_{\text{SWNT}}$ , of about  $4 \cdot 10^{-14}$  F/ $\mu\text{m}$ , is independent on the total real resistance, however the  $C_{\text{SWNT}}$  value is larger than that theoretically predicted quantum capacitance of a perfect tube. Our observations also indicate that the damping frequency is lower than the theoretically predicted in SWNTs.

**Keywords** – Carbon Nanotubes, Impedance, Quantum Capacitance.

### I. INTRODUCTION

Single wall carbon nanotubes (SWNT) are being considered the potential building blocks of electronic devices that can be scaled down to nano-dimensions. Nanotubes are rolled-up sheets of graphite. Depending on the rolling-up direction of the sheet i.e. the chirality vector, they can be either metallic or semiconducting [1]. Semiconducting nanotubes can function as active channels in nanoscale transistors [2, 3] while the metallic ones show promise as nanoscale interconnections and antennas [4, 5]. Compared to the traditional metallic interconnections SWNTs are quasi-1D structures that promise superior DC and AC conductance [6]. The electrical transport properties of carbon nanotubes are especially attractive since they are not affected by surface scattering or surface roughness when the feature size of the interconnects shrinks. Tight Binding Model simulations of conductance in short carbon nanotubes (25 nm long) predict that the conductance should oscillate between inductive and capacitive characters due to resonant tunneling [7, 8]. This phenomenon should not be apparent in nanotubes significantly longer than 25 nm, where the resonances are washed-out due to charge carriers damping. When the AC

frequency exceeds the critical frequency the conductance should become capacitive [8]. An radio-frequency (RC) circuit model for carbon nanotubes [9] predicts a drop in impedance should occur due to damping of the plasmon wave at a critical frequency  $\omega_c = 1/R_{\text{DC}}C_{\text{QE}}$  where  $R_{\text{DC}}$  is the resistance and  $C_{\text{QE}}$  are the combined quantum and electrostatic capacitance of the tube. Currently, very little is known theoretically or experimentally about the damping mechanism. The experimental impedance measurements on individual, approximately 10  $\mu\text{m}$  long semiconducting tubes showed that below 8 MHz there is a static contact resistance of about 18 k $\Omega$  and a negative capacitance of about -4.5 pF, which was attributed to an electron relaxation at the tube-metal contact junction [9]. Thus, no experimental evidence was found to confirm the intrinsic quantum transport properties predicted by the theoretical models.

In this paper we examine experimentally the impedance of individual SWNTs assembled as a conducting channel of a 3-terminal field-effect-transistor (FET) structure. Our present work is aimed at further elucidating the impedance characteristic in a non-transmission line configuration. This choice is predicated on previous findings that the impedance of nanostructures is largely determined by the dielectric polarizability of carbon nanotubes [10].

### II. MATERIALS AND MEASUREMENTS

Purified SWNTs were purchased from BuckyUSA Company. SWNTs were suspended in a 1 % by mass fraction aqueous solution of sodium dodecyl sulfate (SDS) followed by sonification and a centrifugation process, and then assembled on Platinum electrodes using dielectrophoresis [11]. The test structure was patterned on a highly doped Si substrate with a silicon oxide layer of 500 nm in thickness using photo-lithography. This structure can work as a FET. The distance between the electrodes (the channel length) was between 0.5  $\mu\text{m}$  to about 2.0  $\mu\text{m}$ . We applied an AC electric field of 10 Vp-p and a frequency of 5 MHz between the control electrodes to obtain well-aligned individual SWCNTs. Fig. 1 illustrate an individual SWNT assembled in the 2  $\mu\text{m}$  channel. To remove SDS from the surfaces of the nanotubes after dielectrophoresis, the substrates with aligned nanotubes were soaked in deionized water for 15 min to 20 min, rinsed with de-ionized water, and dried under flowing nitrogen gas [11]. Contacts to test

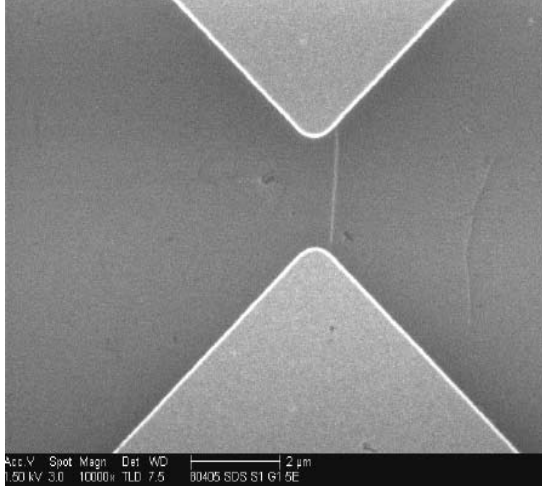


Fig. 1. Individual SWNT assembled on the test structure. The tube length is about 2  $\mu\text{m}$ .

structure were made using 4T coaxial micro probes, DCP 115R, from Cascade Microtech on a Cascade Probe Station.

Measurements of complex impedance (impedance magnitude  $Z^*$  and the corresponding phase angle,  $\theta$ ) were conducted in the frequency range  $f$  of 40 Hz to 110 MHz through a four-terminal technique using an Agilent 4294A Precision Impedance Analyzer. The analyzer was calibrated according to the manufacturer specification, and then the test fixture was compensated to a 50  $\Omega$  load standard, which was obtained from Cascade.

Fig. 2 illustrates the measurement when probes are in contact with the 2  $\mu\text{m}$  channel. The combined relative

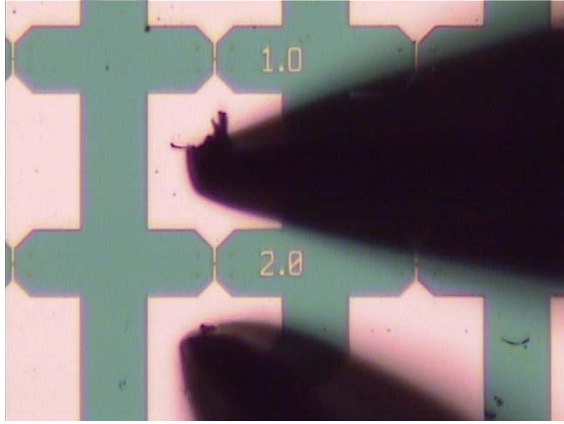


Fig. 2. Contacts to test structure were made using 4T coaxial probes on a Cascade Probe Station.

experimental uncertainty of the measured complex impedance magnitude was within 2 %, while the relative experimental uncertainty of the phase angle measurements was about 1 %.

### III. RESULTS AND DISCUSSION

The results of the impedance measurements at an AC amplitude of 100 mV are illustrated in Figure 3 where the impedance magnitude is plotted as a function of frequency at several DC-bias values. Line (1) in Fig. 3 represents impedance of the test structure measured without SWNT,  $Z = 1/2\pi f C_0$ , with typical  $C_0$  value between 11 fF to 15 fF. The plateau seen in each plot extending up to a certain frequency ( $f_c$ ) corresponds to the real resistance ( $R_0$ ).

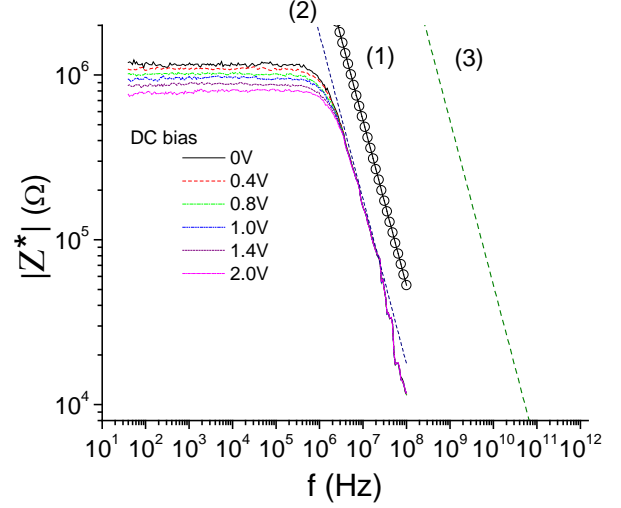


Fig.3. Impedance of SWNT as a function of frequency under DC Bias. The lines represent: (1) –  $C_0$ , (2) –  $C_m$  and (3) –  $C_{QE}$ .

The resistance values are approximately symmetric in respect to  $\pm$  DC bias indicating symmetric contacts. It is seen that  $R_0$  decreases with increasing bias from 1.2 M $\Omega$  at 0V to about 0.8 M $\Omega$  at 2V. Assuming that within the applied DC-voltage range the SWNT conductivity is linear, the observed voltage dependence of  $R_0$  can be attributed to forward-biased Schottky barriers at each contact. Fig 3 indicates that the test structure with SWNT can be represented as a lumped RC circuit consisting of  $R_0$  and complex capacitance  $C_m^*$ . The equivalent complex impedance of such circuit is the sum of the admittances of the two elements.

$$Z^* = [(1/R_0) + j2\pi f C_m^*]^{-1} \quad (1)$$

From Fig. 3 and Eq. (1) it is apparent that when frequency  $f$  is sufficiently high, the overall impedance is dominated by the circuit capacitance  $C_m$ . This effect is seen in Fig. 3 as a linear scaling of  $|Z^*|$  with frequency with a slope of  $C_m$ . Thus we can determine the circuit real capacitance,  $C_m$ , (Fig 3 line 2) and then estimate  $C_{SWNT} = C_m - C_0$ . The crossover frequency ( $f_c$ ) is determined by the time constant of the RC circuit,

approximately a point in Fig. 3 at which  $R_0$  crosses the plot  $Z=1/2\pi f C_{SWNT}$ :

$$f_c = 1/(2\pi R_0 C_{SWNT}) \quad (2)$$

It is seen that  $f_c$  is about 2.5 MHz when  $R_0$  drops to about 800 k $\Omega$  at  $V_{DC}$  of 2 V (Fig. 3).

Since the forward-biased contact barriers contribute to the measured  $R_0$  it is difficult to extract the intrinsic resistivity of SWNT. Model calculations suggest that the theoretical value of characteristic impedance for a ‘non-interacting’ SWNT is about 12.5 k $\Omega$ , which in a high-damping limit may correspond to  $R_0$  of about 100 k $\Omega$  [9]. We estimate that when treated as a resistive termination, our SWNT circuit would reach this level of impedance at an unrealistic bias level of over 100V. In contrast, the total capacitance of the circuit  $C_m$  is about  $10^{-13}$  F regardless of the bias level, and thus, we can estimate  $C_{SWNT}$  to be about  $4 \cdot 10^{-14}$  F/ $\mu$ m. For metallic SWNTs with the Fermi velocity ( $v_F$ ) of the charge carriers approximate to that of perfect graphene, the theoretical value of quantum and electrostatic capacitance combined ( $C_{QE}$ ) is predicted to be in the range of  $10^{-16}$  F/ $\mu$ m [9]. Within this formalism we may estimate that  $v_F$  for our SWNT is about  $10^3$  m/s, which is about two orders of magnitude below  $v_F$  of a perfect tube. This estimate is not unreasonable for a real SWNT with defects. A variety of different materials with nano-scale structure and partially metallic conductivity show surprisingly similar behavior. The generic quantum-analytic approximations for such structures can be extended to include defect-induced fluctuations in tunneling between conducting regions separated by thin barriers. Results shown in Fig. 3 agree qualitatively with the low frequency impedance characteristic of a perfect metallic SWNT. In particular the frequency range at which the impedance characteristics becomes capacitive (Eq.2) agrees reasonably well with the nanotube dynamic impedance predicted for the over-damped mode.

#### IV. CONCLUSION

Impedance of individual SWCNT at the low frequency range is the resistance of the tube with contact resistance. We observe a sharp conductor to insulator transition at a crossover frequency above which the circuit response becomes capacitive. The crossover frequency, above which the impedance begins to decrease, is given by the time constant of the RC circuit, proportional to the inverse of the  $R_0 C_{SWNT}$  term. The extracted from the circuit capacitance,  $C_{SWNT}$ , is significantly larger than that theoretically predicted  $C_{QE}$ . However our results agree qualitatively with the low frequency impedance characteristic of metallic SWNTs. Furthermore, our results imply that the crossover frequency due to quantum capacitance of a perfect SWNT would fall in the range of about 100 GHz.

#### ACKNOWLEDGMENT

This work was supported in part by the NIST Carbon Nanotube Competence Program.

#### DISCLAIMER

Certain equipment, instruments or materials are identified in this paper in order to adequately specify the experimental details. Such identification does not imply recommendation by the National Institute of Standards and Technology nor does it imply the materials are necessarily the best available for the purpose.

#### REFERENCES

- [1] R. Saito, G. Dresselhaus, M. S. Dresselhaus, “Physical Properties of Carbon Nanotubes”, Imperial College Press, London (2003).
- [2] J. Tersoff, M. Freitag, J. C. Tsang and P. Avouris, “Device modeling of long-channel nanotube electro-optical emitter”, J. Appl. Phys. Lett., **86**, 263108 (2005).
- [3] X. Zhou, J. Park, S. Huang, J. Liu and P. L. McEuen, “Band Structure, Phonon Scattering, and the Performance Limit of Single-Walled Carbon Nanotube Transistors, Phys. Rev Lett., **95**, 146805-1 (2005).
- [4] Z. Yu and P. J. Burke, “Microwave transport in metallic single-walled carbon nanotubes” Nano Lett., **5**, 1403-1406 (2005).
- [5] G. W. Hanson, “Fundamental Transmitting Properties of Carbon Nanotube Antennas”, IEEE Trans. Antennas and Propagation, **53**, 3426-3435 (2005).
- [6] S. Frank, P. Poncharal, Z. Wang and J. H. de Heer, “Science, **280**, 1744 (1998).
- [7] D. Orlikowski, H. Mehrez, J. Taylor, H. Guo, J. Wang, and C. Roland, “Resonant transmission through finite-sized carbon nanotubes”, Phys. Rev. B, **65**, 155412 (2001).
- [8] Y. He, D. Hou, X. Liu, C. Fun and R. Han, “AC conductance of finite-length carbon nanotubes”, J. Phys. Condens. Matter, **18**, 8707-8713 (2006).
- [9] P. J. Burke, “An RF Circuit Model of Carbon Nanotubes”, IEEE Trans. Nanotechnology, **2**, 55-58 (2000)
- [10] F. Leonard, J. Tersoff, Dielectric Response of semiconducting carbon nanotubes” Appl. Phys. Lett., **81**, 4835-4837 (2002).
- [11] L.F. Dong, V. Chirayos, J. Bush, J. Jiao, V. M. Dubin, R. V. Chebrian, Y. Ono, J. F. Conley, Jr., and B.D. Ulrich, “Floating-Potential Dielectrophoresis Controlled Fabrication of Single Carbon Nanotube Transistors and Their Electrical Properties,” J. Phys. Chem. B, **109**, 13148-13153 (2005).